This article has been accepted for publication in a future issue of this journal, but has not been fully edited. Content may change prior to final publication. Citation information: DOI 10.1109/JBHI.2019.2956604, IEEE Journal of Biomedical and Health Informatics

Noninvasive Cardiac Output and Central Systolic Pressure from Cuff-Pressure and Pulse Wave Velocity: A Model-Based Study

Vasiliki Bikia, Stamatia Pagoulatou, Bram Trachet, Dimitrios Soulis, Athanase D. Protogerou, Theodore G. Papaioannou, Nikolaos Stergiopulos

Abstract— ***Goal:*** **We introduce a novel approach to estimate cardiac output (CO) and central systolic blood pressure (cSBP) from noninvasive measurements of peripheral cuff-pressure and carotid-to-femoral pulse wave velocity (cf-PWV).** ***Methods:*** **The adjustment of a previously validated one-dimensional arterial tree model is achieved via an optimization process. In the optimization loop, compliance and resistance of the generic arterial tree model as well as aortic flow are adjusted so that simulated brachial systolic and diastolic pressures and cf-PWV converge towards the measured brachial systolic and diastolic pressures and cf-PWV. The process is repeated until full convergence in terms of both brachial pressures and cf-PWV is reached. To assess the accuracy of the proposed framework, we implemented the algorithm on in vivo anonymized data from 20 subjects and compared the method-derived estimates of CO and cSBP to patient-specific measurements obtained with Mobil-O-Graph apparatus (central pressure) and two-dimensional transthoracic echocardiography (aortic blood flow).** ***Results:*** **Both CO and cSBP estimates were found to be in good agreement with the reference values achieving an RMSE of 0.36 L/min and 2.46 mmHg, respectively. Low biases were reported, namely -0.04±0.36 L/min for CO predictions and -0.27±2.51 mmHg for cSBP predictions.** ***Significance:*** **Our one-dimensional model can be successfully "tuned" to partially patient-specific standards by using noninvasive, easily obtained peripheral measurement data. The in vivo evaluation demonstrated that this method can potentially be used to obtain central aortic hemodynamic parameters in a noninvasive and accurate way.**

Index Terms—**noninvasive, cardiac output, central pressure, 1-D model, patient-specific models, optimization methods.**

I. Introduction

CENTRAL hemodynamic quantities, such as cardiac output (CO) and central aortic pressure, have been generally shown to be more powerful predictors of clinical outcomes than corresponding measurements obtained in the peripheral arteries such as the radial, femoral or brachial arteries [1], [2]. Critically ill or intensive care unit patients often require continuous assessment of cardiac output for diagnostic purposes or for guiding therapeutic interventions [3]–[5], whereas several studies have shown the pathophysiological importance of central systolic blood pressure (cSBP) as the critical index for diagnosis and preventing cardiovascular diseases [6]–[8]. But despite the diagnostic importance of central measurements, their clinical use is severely hampered by their invasive nature (in case of central pressure) or cost and need of special equipment and training (in case of aortic blood flow). Peripheral measurements such as systolic and diastolic brachial pressure, on the other hand, are noninvasive and can be monitored by any clinician on a regular basis [9]. This has given rise to substantial research efforts to develop noninvasive methods for estimating central cardiovascular hemodynamics from peripheral measurements [10], [11].

The state-of-the-art of methods for obtaining central hemodynamic indices is based on generalized transfer functions (TF) [12]–[14], pulse wave analysis [15]–[17] or parameter estimation from pooled clinical data [18], [19]. None of these techniques accounts for the specific arterial tree properties of each subject [20], [21]. The use of mathematical models constitutes a valuable tool to investigate patient-specific aspects of aortic hemodynamics, which are difficult to assess in clinical practice. Patient-specific modeling is an emerging field which promises to have a significant impact on clinical practice [22]. Data assimilation has significantly promoted patient-specific modeling and has become an area of increasing interest [23], [24].

Prompted by previous work in the field, the hypothesis formed in this study is that central hemodynamic parameters (i.e., CO and cSBP) can be accurately estimated by making better use of the patient-specific information that is embedded in easily obtained noninvasive peripheral cuff-pressure and pulse wave velocity measurements. In contrast to current methods using population-based generalized TFs, this study relies on a generalized one-dimensional (1-D) model which is further partially personalized by using additional measurements of brachial systolic blood pressure (SBP) and diastolic blood pressure (DBP), and carotid-to-femoral pulse wave velocity (cf-PWV). The method developed and presented in this manuscript combines insights from both cardiovascular modeling and data assimilation methodology. This is done by feeding the 1-D model with the minimum number of inputs that allows for the calibrated prediction of the aforementioned central hemodynamic parameters. The proposed framework was

This paragraph of the first footnote will contain the date on which you submitted your paper for review. It will also contain support information, including sponsor and financial support acknowledgment. For example, "This work was supported in part by the U.S. Department of Commerce under Grant BS123456."

The next few paragraphs should contain the authors' current affiliations, including current address and e-mail. For example, F. A. Author is with the National Institute of Standards and Technology, Boulder, CO 80305 USA (e-mail: author@ boulder.nist.gov).

S. B. Author, Jr., was with Rice University, Houston, TX 77005 USA. He is now with the Department of Physics, Colorado State University, Fort Collins, CO 80523 USA (e-mail: author@lamar.colostate.edu).

T. C. Author is with the Electrical Engineering Department, University of Colorado, Boulder, CO 80309 USA, on leave from the National Research Institute for Metals, Tsukuba, Japan (e-mail: author@nrim.go.jp).

This article has been accepted for publication in a future issue of this journal, but has not been fully edited. Content may change prior to final publication. Citation information: DOI 10.1109/JBHI.2019.2956604, IEEE Journal of Biomedical and Health Informatics

evaluated with in vivo data from a population of 20 healthy adults [25]. Estimated values of CO and cSBP were compared to the corresponding CO and cSBP values measured by a noninvasive, validated, automated, oscillometric sphygmomanometer (Mobil-O-Graph) and transthoracic two-dimensional (2-D) echocardiography – Doppler, respectively.

II. Methods and Materials

A. Brief Description of the Generic 1-D Arterial Tree Model

In this study, we adopted a validated 1-D model of the systemic arterial tree that has been previously described by Reymond *et al.* [26]. The arterial tree, as depicted in Fig. 1, includes the main arteries of the systemic circulation, including a detailed network representation of the cerebral circulation and the coronary circulation. In brief, the governing equations of the model are obtained by integration of the longitudinal momentum and continuity of the Navier-Stokes equations over the arterial cross section. Flow and pressure waves throughout the vasculature are obtained by solving the governing equations with proper boundary conditions using an implicit finite-difference scheme. The arterial segments of the model are considered as long tapered tubes, and their compliance is defined by a nonlinear function of pressure and location as proposed by Langewouters [27]. The arterial wall behavior is considered to be nonlinear and viscoelastic according to Holenstein *et al.* [28]. Local arterial compliance is calculated after approximating pulse wave velocity (PWV) as an inverse power function of arterial lumen diameter, following the physiological values reported in the literature. Resistance of the peripheral vasculature is accounted for by coupling the distant vessels with three-element Windkessel models. At the proximal end, the arterial tree either receives a prescribed input aortic flow waveform or is coupled with a time-varying elastance model for the contractility of the left ventricle [29], [30]. Further details on the 1-D model can be found in the original publications [22], [26].

The model has been thoroughly validated [22], [26] and is able to predict pressure and flow waves in good quantitative and qualitative agreement with in vivo measurements, particularly with respect to shape and wave details.

B. Rationale of The Proposed Method

This work applied an optimization algorithm in order to partially adjust the generic 1-D arterial tree model to the specific patient under consideration. The rationale behind this methodology was that adjusting (some of the) model parameters may be sufficient to approximate the measured data [31]. Before the optimization, the aim was to identify the most sensitive parameters which mainly drive the variability of the model output.

In our analysis, peripheral SBP, DBP, and cf-PWV were the model outputs. Our approach was based on the idea that, for any individual with a given set of peripheral SBP, DBP, and cf-PWV values, there will be only one solution for the arterial tree model. Thus, if we simultaneously adjust the properties of the model and the input aortic blood flow to capture a given peripheral cuff-pressure and cf-PWV, then this allows for the calibrated derivation of CO and cSBP. In order to identify and select those highly sensitive parameters, we performed a parameter identifiability analysis [32].

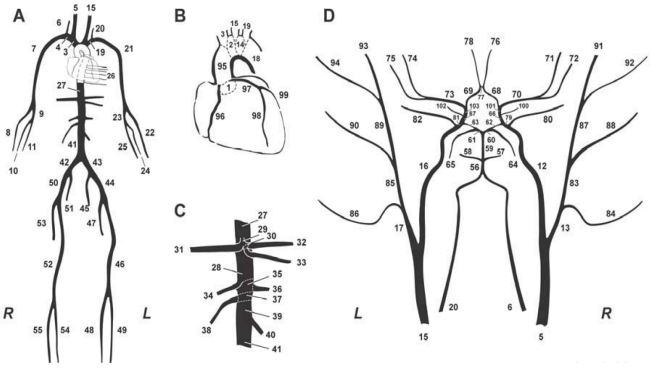

Fig. 1. Schematic representation of the model of systemic circulation developed by Reymond *et al.* [26]. (A) Main systemic arterial tree. (B) Detail of the aortic arch and the coronary network. (C) Detail of the principal abdominal aorta branches. (D) Blown-up schematic of the detailed cerebral arterial tree, which is connected via the carotids (segments 5 and 15) and the vertebrals (segments 6 and 20) to the main arterial tree shown in (A).

TABLE I
Input And Output Parameters of The 1-D Arterial Tree Model

	Corresponding variable	Value
Input parameter		
Blood density	ρ	1050 kg/m
Blood viscosity	μ	0.004 Pa.s
Geometry	`arterial_length, arterial_diameter`	`(no_segments)x1 vector, (no_segments)x1 vector`
Distensibility and terminal compliance	`C`	`(no_segments)x1 vector`
Total peripheral resistance	`R`	`(no_terminal_segments)x1 vector`
Aortic flow[a]	`aortic_flow`	`(no_time_points)x1 vector`
Output		
Pressure waves	`pressures`	`(no_segments)x(no_time_points) vector`
Flow waves	`flows`	`(no_segments)x(no_time_points) vector`

[a]The aortic flow is characterized by three points, namely the Q_{max}, T_{period}, $T_{systole}$). The aortic flow wave shape is considered fixed. no_segments: number of arterial segments, no_time_points: length of the time signal.

C. Parameter Identifiability Analysis

The arterial tree model of this study is fully characterized by its geometry, the distensibility of all arterial segments, and the peripheral impedances (described by terminal compliances and resistances). Additionally, aortic flow is needed as proximal boundary condition. Table I summarizes the input and output parameters of the arterial tree model. For the following analysis, brachial pressure was selected as the peripheral pressure model output. Thus, the three model outputs became brachial SBP (brSBP), brachial DBP (brDBP), and cf-PWV.

The sensitivity matrix $\mathbf{V} = \{\mathbf{v_{ij}}\}$ was calculated for the entire set of parameters in the arterial tree model using the finite difference approximation [33]. Subsequently, the scaled sensitivity matrix was estimated to provide the dimension-free sensitivity information. The scaled sensitivity matrix $\mathbf{S} = \{\mathbf{s_{ij}}\}$ was derived from the following formula:

$$\mathbf{s_{ij}} = \frac{\mathbf{v_{ij}}\boldsymbol{\Delta\theta_j}}{\mathbf{SC_i}}.$$

This article has been accepted for publication in a future issue of this journal, but has not been fully edited. Content may change prior to final publication. Citation information: DOI 10.1109/JBHI.2019.2956604, IEEE Journal of Biomedical and Health Informatics

Here, according to Brun *et al.* [32], $\mathbf{\Delta\theta_j}$ was set equal to the original set of parameters $\boldsymbol{\theta}$, i.e., $\mathbf{\theta_0}$, whereas the optimal choice for $\mathbf{SC_i}$ was the mean value of the experimental observations for each model output (Table II).

The scaled sensitivity matrix is presented below in Fig. 2.

TABLE II
DESCRIPTION OF $\Delta\Theta_J$ AND SC_I PARAMETERS

Parameter	Unit	$\Delta\theta_j = \theta_0$
Qmax	mL/s	436.23
C	mL/mmHg	1.90
Tperiod	ms	790.00
R	mmHg.s/mL	1.00
arterial_length[a]	cm	180.00
arterial_diameter[b]	cm	2.94
Tsystole	ms	270.00

State	Unit	SC_i
Peripheral SBP	mmHg	117.55
Peripheral DBP	mmHg	77.25
Cf-PWV	m/s	6.89

[a]Arterial length is defined with respect to height. The reference state of the arterial tree model corresponds to an individual with a height equal to 180 cm. [b]Arterial diameter is defined with respect to the diameter of the aorta. The alteration of the diameter for the different arteries is done uniformly.

Each element $\mathbf{s_{ij}}$ corresponds to the sensitivity of the model output j = 1, 2, 3, i.e., brSBP, brDBP, and cf-PWV, with respect to changes in the parameter i = 1,…,7, i.e., arterial length, arterial diameter, C, R, T_{period}, $T_{systole}$, Q_{max}.

In order to acquire additional information on the sign and distribution of the values in each column $\mathbf{j}$, $\boldsymbol{\delta}_\mathbf{j}^{\mathbf{msqr}}$ [32] was computed and ranked in decreasing order. The decreasing order of $\boldsymbol{\delta}_\mathbf{j}^{\mathbf{msqr}}$ gave the parameters' importance ranking [32] (Table III). It was observed that Q_{max}, C, T_{period} and R are considered the most sensitive parameters. Since the sensitivities of the rest parameters are not negligible, we chose to approximate them using previously published data (more details are provided in the *D. Tuning of The Generic 1-D Arterial Tree Model* section). We assumed that the approximations do not impose a significant error in the results due to their small sensitivities.

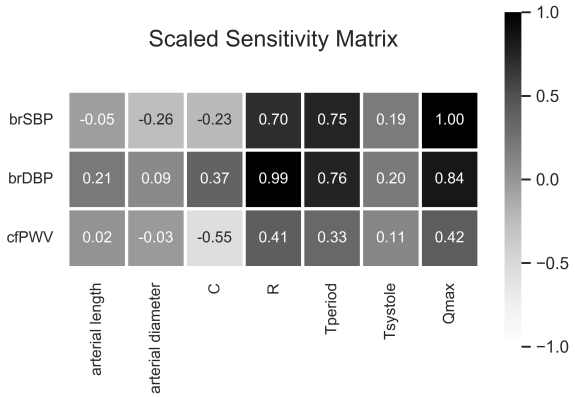

Fig. 2. The scaled sensitivity matrix for the entire set of parameters in the 1-D arterial tree model.

TABLE III
PARAMETER IMPORTANCE RANKING

Parameter	$\boldsymbol{\delta}_\mathbf{j}^{\mathbf{msqr}}$
Qmax	0.52
R	0.48
Tperiod	0.42
C	0.26
Tsystole	0.11
arterial_diameter	0.10
arterial_length	0.08

Based on the aforementioned considerations and the resulted importance ranking, we partitioned the set of parameters $\boldsymbol{\theta}$ into two components $(\boldsymbol{\theta}_\mathbf{K}^\mathbf{T}, \boldsymbol{\theta}_{\tilde{\mathbf{K}}}^\mathbf{T})$ with $\mathbf{K = 3}$, namely:

$$\boldsymbol{\theta}_\mathbf{K}^\mathbf{T} = \{ \text{C, R, } Q_{max} \} ,$$

$$\boldsymbol{\theta}_{\tilde{\mathbf{K}}}^\mathbf{T} = \{\text{arterial\_length, arterial\_diameter, } T_{period}, T_{systole} \} .$$

Only the component $\boldsymbol{\theta}_\mathbf{K}^\mathbf{T}$ was to be estimated from the measured data whereas the component $\boldsymbol{\theta}_{\tilde{\mathbf{K}}}^\mathbf{T}$ (i.e., the remaining parameters) was fixed at a priori value; this is a common practice in identifiability analysis [32]. Concretely, arterial_length was adjusted based on height information, arterial_diameter was determined based on [34], T_{period} was directly assigned the patient's measured HR and $T_{systole}$ was set to a HR-related value according to [35]. The hypothesis was that the subset of parameters, i.e., compliance (C), total peripheral resistance (R), and maximum flow (Q_{max}), can be uniquely estimated from the model outputs, i.e., brSBP, brDBP, and cf-PWV.

In order to verify our hypothesis, we had to confirm that the set $\boldsymbol{\theta}_\mathbf{K}^\mathbf{T}$ was identifiable or, in other words, that $\boldsymbol{\theta}_\mathbf{K}^\mathbf{T}$ was sufficient to detect the variability in the model output (i.e., brSBP, brDBP, and cf-PWV). If $\boldsymbol{\theta}_\mathbf{K}^\mathbf{T}$ is classified as identifiable, then we can deduce that brSBP, brDBP, and cf-PWV can estimate $\boldsymbol{\theta}_\mathbf{K}^\mathbf{T}$ in a unique way.

The joint influence of the parameters $\boldsymbol{\theta}_\mathbf{K}^\mathbf{T}$ parameters on the model output was considered. To this respect, the collinearity of parametric sensitivity was used [32]. To calculate collinearity, we first normalized the scaled sensitivities $\tilde{\mathbf{S}}$ and we defined the collinearity index $\boldsymbol{\gamma}_\mathbf{K}$ as follows:

$$\boldsymbol{\gamma}_\mathbf{K} = \frac{\mathbf{1}}{\mathbf{min}_{||\mathbf{b}||=\mathbf{1}}||\widetilde{\mathbf{S_K}}\boldsymbol{\beta}||} = \frac{\mathbf{1}}{\sqrt{\boldsymbol{\lambda}_\mathbf{K}}},$$

where $\widetilde{\mathbf{S_K}}$ is the submatrix of the normalized sensitivity matrix that consists of the columns that correspond to $\boldsymbol{\theta}_\mathbf{K}^\mathbf{T}$, and $\boldsymbol{\lambda}_\mathbf{K}$ is the smallest eigenvalue of $\widetilde{\boldsymbol{S}_\boldsymbol{K}^\boldsymbol{T}}\widetilde{\mathbf{S_K}}$ [32], [36].

According to Brun *et al.* [32], a subset of parameters can be classified as identifiable if the collinearity index $\boldsymbol{\gamma}_\mathbf{K}$ is smaller than 20. In our analysis, $\boldsymbol{\gamma}_\mathbf{K}$ was found to be equal to 6.90 and thus, we deduced that there is a unique solution of model

This article has been accepted for publication in a future issue of this journal, but has not been fully edited. Content may change prior to final publication. Citation information: DOI 10.1109/JBHI.2019.2956604, IEEE Journal of Biomedical and Health Informatics

parameters for a given set of model outputs (i.e., brSBP, brDBP, and cf-PWV).

D. Tuning of the Generic 1-D Arterial Tree Model

After proving the validity of our primary hypothesis, the following step was to find the adjusted input model parameters that produce as output the given measured data (i.e., brachial SBP and DBP, and cf-PWV). In this respect, the global compliance and global peripheral resistance of the entire arterial tree as well as the input aortic flow were adjusted. This was done by multiplying the compliance of each arterial segment by a common scaling factor. Similarly, a different scaling factor was used to adjust all peripheral resistances. Finally, Q_{max} was modified by multiplication with a third scaling factor. An optimization algorithm was employed to derive the optimal distensibility, resistance and aortic flow scaling factors. Once the "tuning" was completed, the 1-D model used the adjusted parameters and produced the flow and pressure waves for every segment of the arterial tree. From the solution, we were able to obtain the flow and pressure at the aorta, namely to compute the CO and cSBP.

In this approach, the distensibility and the terminal compliance (C) of each arterial segment were modified in a uniform way for young individuals. For older or hypertensive subjects, stiffening was considered as nonuniform and more pronounced in the proximal aortic path [37]. The importance of age-related nonuniform aortic stiffening for central hemodynamics and wave reflections has been demonstrated in previous studies [38]. In order to account for this, data for the age-related local nonuniform aortic stiffening were obtained from [39]. The nonuniform stiffening of the aorta was considered by changing the relative regional distensibility of the proximal aorta (segments 1-95-2-14-18-27 of the arterial tree in Fig. 1) through multiplication with an age-related proximal factor (Fig. 3). Therefore, two scaling factors were considered: a global scaling factor multiplied with all arterial compliances and a proximal scaling factor that was additionally multiplied with only the compliance of the proximal aorta. This was to satisfy the relative relation between the proximal distensibility and the peripheral distensibility. Fig. 3 reports the scaling factors with respect to age. The goodness of fit was high with a coefficient of determination, R^2, equal to 0.99.

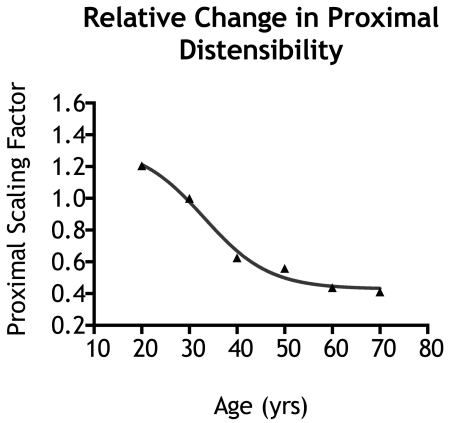

Fig. 3. The proximal scaling factor with respect to age for adjusting the relative distensibility of the proximal aorta.

Resistance (R) was altered in a uniform way for all terminal vessels in the model. Aortic flow was prescribed as an uncalibrated generic physiological wave, which was scaled with respect to amplitude and time during the adjustment process. The geometry of the arterial vessels (i.e., arterial_length and arterial_diameter) was adjusted based on the age, gender, height, and body surface area (BSA) of each subject. For this purpose, data which associate aortic diameter size with age, gender and BSA were used from previous studies [34]. The length of the generic arterial tree segments was normalized and, subsequently, was multiplied by a scaling factor so as to be adjusted to the height of each subject. This concept was implemented in an iterative optimization process. The reason for employing an optimization process was to avoid searching the entire input model parameters space.

E. Optimization Process

A schematic representation of the optimization algorithm is shown in Fig. 4. In the first optimization iteration the structure of the algorithm was as follows: an uncalibrated generic aortic

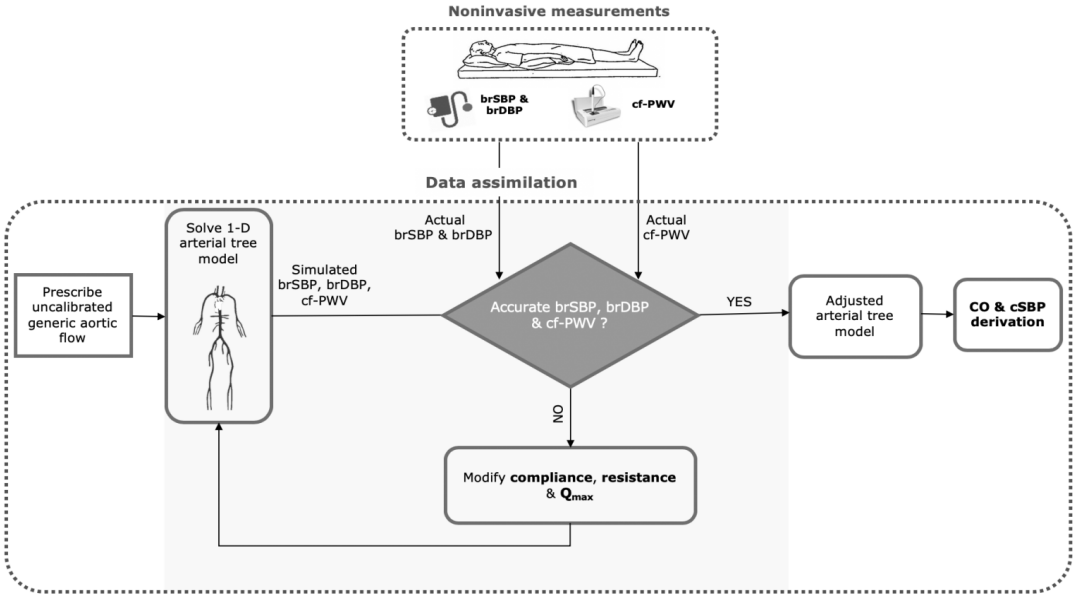

Fig. 4. Schematic representation of the optimization process for predicting noninvasive cardiac output and central systolic blood pressure. brSBP: brachial systolic blood pressure, DBP: brachial diastolic blood pressure, cf-PWV: carotid-to-femoral pulse wave velocity, CO: cardiac output, cSBP: central systolic blood pressure.

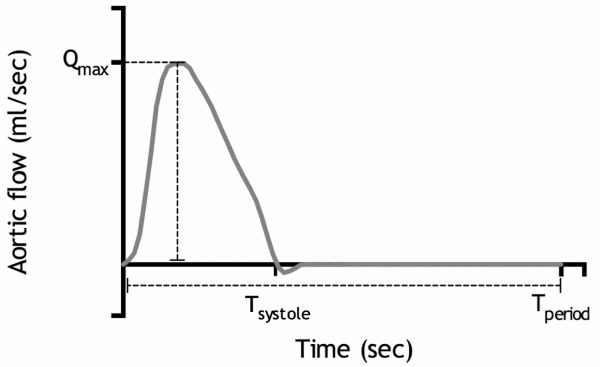

Fig. 5. Uncalibrated generic aortic flow waveform that is used as input to the 1-D arterial tree solver.

flow curve was used as initial input to the model (Fig. 5). For the generic uncalibrated aortic flow, an "average" physiologically shaped wave was selected. The scaling was performed based on the adjustment of three characteristic values, i.e., the velocity peak (Q_{max}), time period (T_{period}), and systolic duration ($T_{systole}$) (Fig. 5). The T_{period} of the uncalibrated aortic wave was adjusted with respect to the measured HR. Previously published data on the HR-related changes in systolic duration [35] were used to adapt the $T_{systole}$ with respect to the given HR. Therefore, only Q_{max} remained to be optimized. A random Q_{max}, and therefore SV, was selected for the initial aortic flow input. The 1-D model subsequently computed all flows and pressures throughout the arterial tree, including the measured variables (brachial SBP and DBP, cf-PWV) as well as the unknown quantities of interest (CO, cSBP). The model was expected to produce an inaccurate prediction of flows and pressures due to inaccurate model parameters and the inaccurate input aortic flow for the specific subject under investigation. Similarly, the calculated cf-PWV was likely not the same as the measured cf-PWV. To address this issue, the noninvasive, patient-specific measurements were integrated into the model using a gradient-based optimization algorithm. The reference compliance, resistance and Q_{max} of the generic arterial tree were adjusted by multiplication with different scaling factors until brachial SBP, DBP, and cf-PWV were correctly predicted for the uncalibrated input aortic flow (Fig. 5). Scaling factors for the compliance were chosen so that a range of [0.1, 3.8] mL/mmHg was covered for total arterial compliance. These values correspond to an extensive range of arterial tree stiffness values [27], [40]. The reference total peripheral resistance in the model was 1 mmHg.s/mL. The scaling factor (which was multiplied with the reference resistance) varied within [0.40, 2.00] in order to cover normal values of total peripheral resistance (e.g., [0.40, 2.00] mmHg.s/mL) [41]. For scaling Q_{max}, the scaling factors were chosen so as the corresponding cardiac output is within [2.00, 8.00] L/min [42]. The limits were chosen so that the corresponding quantities as well as the pressure and flow values generated by the arterial tree model comply with physiological hemodynamic conditions. It is to be emphasized that all parameter ranges were wider than what is to be physiologically expected, in order provide the optimization algorithm with sufficient solution space. The optimization loop ran and the process was repeated until convergence in terms of both brachial pressure and cf-PWV was reached. The tolerated error for capturing brachial SBP and DBP was set to 0.01 %, whereas for cf-PWV value it was 0.01 %. A maximum number of iterations ($N_{iter}^{MAX} = 100$) was also defined for each optimization process. If the algorithm did not converge, the process was repeated starting from a different initial solution. In order to ensure that the algorithm was not stalled by a local minimum, several runs starting from a different random initial solution were performed.

F. Model-derived Pulse Wave Velocity

PWV was derived using the tangential method [43]. The method uses the intersection point of two tangents on the arterial pressure wave as a characteristic marker. The first tangent is defined as the line that passes tangentially through the initial systolic upstroke, i.e., the maximum of the first derivative. The second tangent line is the horizontal line passing through the minimum pressure point. Since our cohort study consists of cf-PWV data, the method was applied to estimate the pulse transit time (PTT) between the carotid artery and the femoral artery. Total aortic length was determined by

summation of the lengths of the arterial segments within the transmission path, i.e., the relevant carotid-to-femoral path (segments 5-3-2-14-18-27-28-35-37-39-41-42-44 of the generic arterial tree in Fig.1). Finally, the value of cf-PWV was calculated by dividing the total length by the PTT.

III. Measurement Protocol

A preliminary assessment of the proposed methodology was carried out by testing the predictions of the method against in vivo data previously collected by Papaioannou *et al.* [25]. The study population included twenty-four subjects who were referred for noninvasive cardiovascular risk assessment. Subjects with risk factors or those receiving medication were also enrolled. Patients with aortic valve disease or arrhythmias were excluded. The measurement protocol has been approved by the Scientific Board of Laikon General Hospital (Reference no: E53610/7/2013).

For each subject, brachial pressure waves were recorded at the brachial artery by oscillometric sphygmomanometry using the Mobil-O-Graph device (I.E.M. GmbH, Stolberg, Deutschland) [44], [45]. Central pressure waves were extracted by mathematical transformation of brachial pressure waves [46]. Carotid-to-femoral pulse wave velocity (cf-PWV) was computed using the SphygmoCor apparatus (AtCor Medical Pty Ltd, West Ryde, Australia). Pressure waves were recorded at the carotid and femoral artery by applanation tonometry (Millar SPT-301, Millar Instruments, TX, USA) as previously described [25]. SphygmoCor also provided recordings of the radial pressure waves [47] and was subsequently used for acquiring the aortic pressure waves [48] through the use of a generalized transfer function. Despite the fact that both devices yield equally precise estimates, in the analysis we made use of the data measured with the Mobil-O-Graph in order to ensure that brachial and aortic pressure were recorded simultaneously. Concretely, the brachial pressure data were used as input variables to the method and the corresponding central pressure data, measured using the same device, were used for the validation. Nevertheless, for the sake of completeness of this work, a second analysis using the SphygmoCor-derived pressure data was performed.

Two measurements of the aortic peak velocity profile at the ascending aorta were performed via transthoracic two-dimensional echocardiographic examination [25]. For this study's simulations, the average of the two measured signals was used. Aortic diameters were extracted from Doppler M-mode and CO was computed by applying the Witzig-Womersely theory [49] considering the profile of peak velocity. Cross-sectional area was assumed to be constant.

All the recorded waveforms were exported as raw data and subject to additional preprocessing. For further details on the measurements protocol, the reader is referred to the original publication [25].

IV. Validation Of The Method-Derived Estimations

Out of the 24 subjects, four were excluded from the study due to unreliable or insufficient data. The population samples included both women (n=9) and men (n=11) and covered an age range of 38.1±12.6 years. For each subject, the processed data from the recordings were used and the previously described methodology was adopted. The descriptive values of the hemodynamic parameters and clinical characteristics of the study population (n=20) are reported in Table IV.

We first implemented the method using as input the peripheral pressure data from the Mobil-O-Graph device. The

TABLE IV
DESCRIPTIVE HEMODYNAMIC PARAMETERS AND CLINICAL CHARACTERISTICS OF THE STUDY POPULATION (N=20)

Index	min	max	mean	SD	min	max	mean	SD
	Women (n=9)				**Men (n=11)**			
Age (years)	27.00	61.00	36.25	11.30	23.00	70.00	39.83	15.30
Height (cm)	152.00	178.00	165.67	8.43	170.00	192.00	179.91	6.93
Weight (kg)	49.00	80.00	61.89	12.17	71.00	128.00	92.27	17.70
Central SBP (mmHg)	93.00	117.00	103.11	8.24	99.00	136.00	117.45	10.71
Brachial SBP (mmHg)	98.00	121.00	110.00	8.05	107.00	145.00	123.73	10.77
Brachial DBP (mmHg)	60.00	81.00	70.67	6.24	74.00	98.00	82.64	7.61
Brachial PP (mmHg)	32.00	46.00	39.33	4.33	33.00	52.00	41.09	5.86
MAP (mmHg)	72.67	94.00	83.78	6.59	85.00	110.33	96.33	8.34
Mean aortic flow (L/min)	3.00	5.40	4.24	0.74	3.00	6.20	4.41	1.01
HR (bpm)	51.00	84.00	70.11	10.40	51.00	89.00	71.45	10.88
cf-PWV (m/s)	5.25	9.05	6.11	1.17	5.40	11.25	7.53	2.21
Smoking (%)		44.44				63.64		
Diabetes (%)		0.00				18.18		
Hypertension (%)		0.00				36.36		
Dyslipidemia (%)		0.00				36.36		
Renal disease (%)		0.00				9.09		
CVD (%)		0.00				36.36		
Stroke (%)		0.00				9.09		
History of CVD (%)		44.44				9.09		

SBP: systolic blood pressure, DBP: diastolic blood pressure, PP: pulse pressure, MAP: mean arterial pressure, HR: heart rate, cf-PWV: carotid-to-femoral pulse wave velocity, CVD: cardiovascular disease.

model CO estimates were compared to the in vivo measurements via transthoracic echocardiography, whereas the predicted cSBPs were evaluated against the respective Mobil-O-Graph central pressure data.

Then, the process was repeated using as input the peripheral pressure data from SphygmoCor. Similarly, COs were validated using as reference the transthoracic echocardiographic data and cSBP predictions were compared versus the in vivo measurements from the respective SphygmoCor-derived central pressure data.

V. Statistics

The agreement, bias and precision between the method-derived predictions and the in vivo data were evaluated by using the Pearson's correlation coefficient (r), intraclass correlation coefficient (ICC), the Bland-Atman analysis and the root mean square error (RMSE). The statistical analysis was performed using the software package Prism (Prism 6, GraphPad Software Inc., San Diego, USA).

VI. Sensitivity to Measurement Errors

In order to assess the sensitivity of the method to errors in the measurements of brachial pressure and the cf-PWV, the analysis was repeated on the entire study population after (i) decreasing the brachial systolic blood pressure with 10 % and (ii) increasing the brachial systolic blood pressure with 10 %. In a similar approach, the effect of overestimating and underestimating the cf-PWV value with 10 % was also examined.

VII. Results

The comparisons between the model-derived estimations and the reference data are presented below.

A. Comparison of Model-derived CO Estimates to the Reference Method

Fig. 6A shows the comparison between the model CO estimates and the in vivo measurements via transthoracic echocardiography using the pressure data from the Mobil-O-Graph device. The corresponding Bland-Altman plot is depicted in Fig. 6B. The RMSE was found to be equal to 0.36 L/min. In 55 % of the cases, the difference between model-CO and reference CO was found to be below 0.3 L/min. Parameters of accuracy, correlation and agreement of CO estimation by the method in comparison to the reference method are summarized in Table V.

Fig. 7A shows the model-predicted CO values compared to the in vivo echocardiographic CO values using the SphygmoCor pressure data. The Bland-Altman plot is given in Fig. 7B. The RMSE was 0.81 L/min and the Pearson's correlation coefficient was equal to 0.73 (Table V). The difference between model-CO and reference CO was less than 0.3 L/min for the 25 % of the cases.

This article has been accepted for publication in a future issue of this journal, but has not been fully edited. Content may change prior to final publication. Citation information: DOI 10.1109/JBHI.2019.2956604, IEEE Journal of Biomedical and Health Informatics

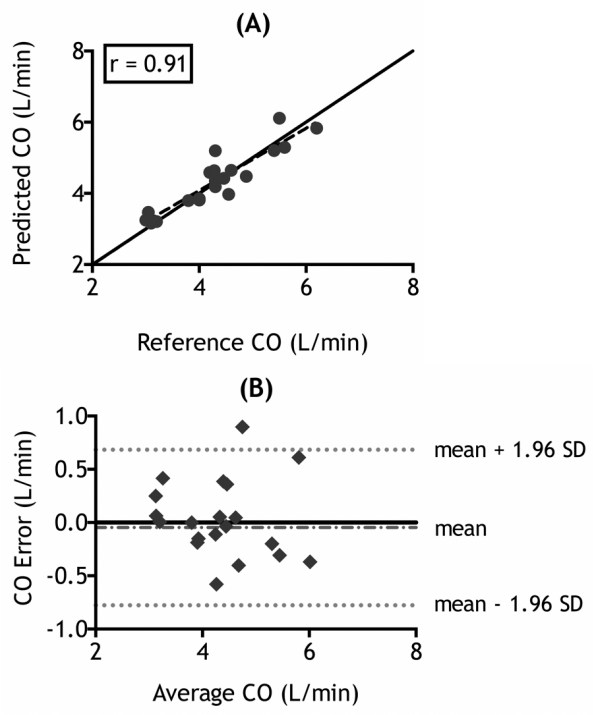

Fig. 6. Comparison of CO values as predicted by the method with the reference in vivo data (using the Mobil-O-Graph pressure data). (A) Scatter plot between the values of CO derived from the method and the values of CO measured with 2-D transthoracic echocardiography (solid and dashed line represent equality and linear regression, respectively). (B) Bland-Altman plot for CO prediction by the model versus 2-D transthoracic echocardiographic measurement. Limits of agreement are defined by the two horizontal dotted lines.

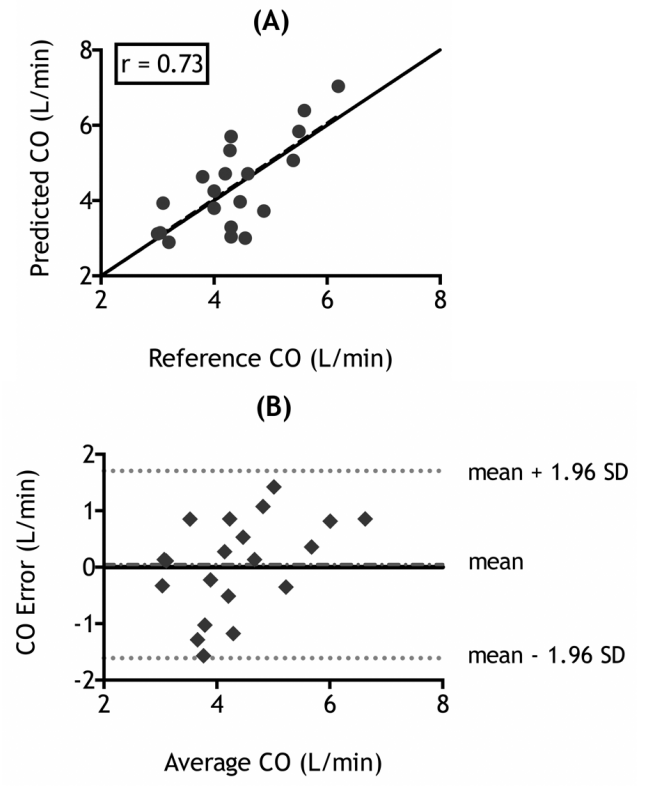

Fig. 7. Comparison of CO values as predicted by the method with the reference in vivo data (using the SphygmoCor pressure data). (A) Scatter plot between the values of CO derived from the method and the values of CO measured with 2-D transthoracic echocardiography (solid and dashed line represent equality and linear regression, respectively). (B) Bland-Altman plot for CO prediction by the model versus 2-D transthoracic echocardiographic measurement. Limits of agreement are defined by the two horizontal dotted lines.

TABLE V
PARAMETERS OF ACCURACY, CORRELATION AND AGREEMENT OF CO ESTIMATION BY THE MODEL IN COMPARISON TO THE REFERENCE METHOD

Parameter	Value (using the Mobil-O-Graph pressure data)	Value (using the SphygmoCor pressure data)
Mean difference (L/min)	0.04	0.04
Standard deviation of difference (L/min)	0.36	0.83
Limits of agreement (L/min)	[-0.68, 0.75]	[-1.61, 1.71]
Root mean square error (L/min)	0.36	0.81
Pearson's correlation coefficient	0.91	0.73
Intraclass correlation coefficient	0.91	0.69

B. Comparison of Model-derived cSBP Estimates to the Reference Method

The scatterplot between the noninvasive cSBP predictions versus the in vivo measurements from the Mobil-O-Graph is presented in Fig. 8A. The method yielded an accurate estimation of cSBP, with a RMSE of 2.46 mmHg, a Pearson's correlation coefficient of 0.98 and a high ICC of 0.98. The Bland-Altman analysis, as given in Fig. 8B, showed a good agreement between the model and the reference cSBP values. The difference between model-cSBP and reference cSBP was less than 1.5 mmHg for the 30 % of the cases, whereas in 60 % of them it ranged between 1.5 and 3.5 mmHg and only 10 % exceeded the 3.5 mmHg. Parameters of precision, correlation and agreement between the estimates and the real values are reported in Table VI.

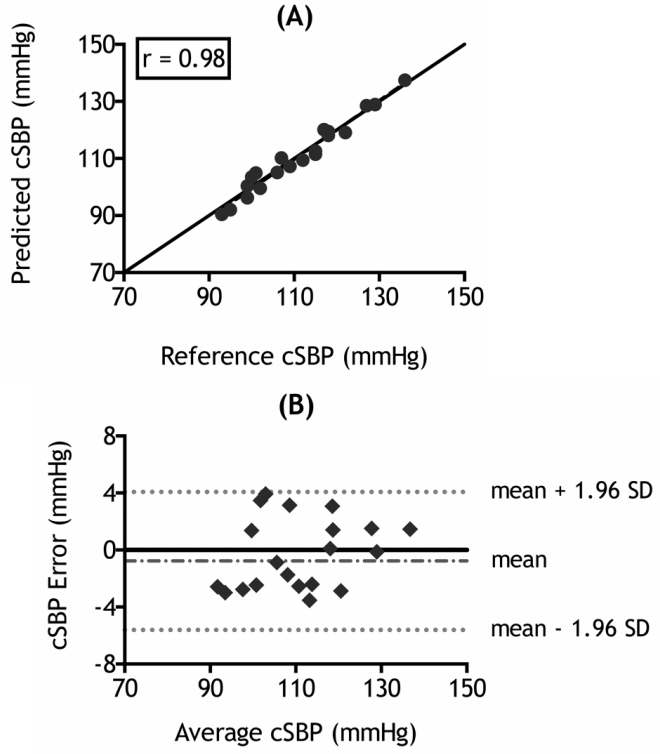

Fig. 8. Comparison of cSBP values as predicted by the model with the reference in vivo data (using the Mobil-O-Graph pressure data). Scatter plot between the values of cSBP derived from the model and the values of cSBP measured with Mobil-O-Graph (solid and dashed line represent equality and linear regression, respectively). (B) Bland-Altman plot for cSBP prediction by the model versus in vivo measurement using the Mobil-O-Graph device. Limits of agreement are defined by the two horizontal dotted lines.

Fig. 9A shows the cSBP predictions compared to the in vivo SphygmoCor cSBP values. The Bland-Altman plot is presented in Fig. 9B. The RMSE was calculated to be 3.42 mmHg and the Pearson's correlation coefficient was equal to 0.98 (Table VI). For 20 % of the cases, the difference between model-cSBP and reference cSBP was less than 1.5 mmHg, for 40 % of them it ranged between 1.5 and 3.5 mmHg and for the remaining 40 % it was found to be above 3.5 mmHg.

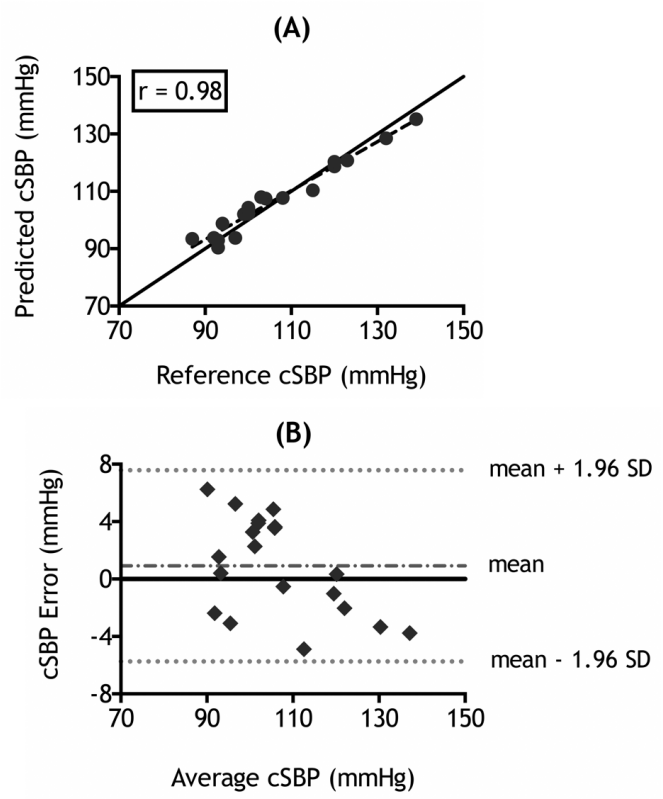

Fig. 9. Comparison of cSBP values as predicted by the model with the reference in vivo data (using the SphygmoCor pressure data). Scatter plot between the values of cSBP derived from the model and the values of cSBP measured with SphygmoCor (solid and dashed line represent equality and linear regression, respectively). (B) Bland-Altman plot for cSBP prediction by the model versus in vivo measurement using the SphygmoCor device. Limits of agreement are defined by the two horizontal dotted lines.

TABLE VI
PARAMETERS OF ACCURACY, CORRELATION AND AGREEMENT OF CSBP ESTIMATION BY THE MODEL IN COMPARISON TO THE REFERENCE METHOD

Parameter	Value (using the Mobil-O-Graph pressure data)	Value (using the SphygmoCor pressure data)
Mean difference (mmHg)	-0.27	0.82
Standard deviation of difference (mmHg)	2.51	3.41
Limits of agreement (mmHg)	[-5.19,4.65]	[-5.75,7.58]
Root mean square error (mmHg)	2.46	3.42
Pearson's correlation coefficient	0.98	0.98
Intraclass correlation coefficient	0.98	0.97

C. Sensitivity of Model Predictions to Input Parameter Measurement Errors

Table VII shows the sensitivity of the model predictions in terms of CO and cSBP when a ±10% error is introduced in the measurements of brachial SBP and cf-PWV.

TABLE VII
ESTIMATES OF RELATIVE ERRORS IN CO AND CSBP AFTER INTRODUCING: (I) A ±10 % ERROR IN THE BRACHIAL SBP MEASUREMENT AND (II) A ±10 % ERROR IN THE CF-PWV MEASUREMENT

Introduced error	CO estimate error (%) *mean±SD*	cSBP estimate error (%) *mean±SD*
+10 % brSBP	26.76±17.01	8.98±5.45
-10 % brSBP	-20.67±18.11	-11.88±4.28
+10 % cf-PWV	-12.73±6.23	-4.34±4.41
-10 % cf-PWV	11.84±9.56	-3.74±4.03

brSBP: brachial systolic blood pressure, cf-PWV: carotid-to-femoral pulse wave velocity, CO: cardiac output, cSBP: central systolic blood pressure, SD: standard deviation.

In case of an overestimation of the brachial SBP, it was noted that CO and cSBP estimates were sensitive to the erroneously measured brachial SBP with relative (with respect to the actual value) errors of 26.76±17.01 % and 8.98 ±5.45 %, respectively. When an underestimation of the brachial SBP was assumed, the errors in CO and cSBP were calculated to be -20.67±18.11 % and -11.88±4.28 %, respectively.

Likewise, a deliberate error of ±10% was imposed to the cf-PWV measurement. The algorithm was reemployed for the new input. The cSBP prediction seems to be more robust to errors in cf-PWV measurements than to errors in brachial blood pressure measurements (Table VII). A ±10 % error in the in vivo cf-PWV rendered small errors in the cSBP estimations, equal to -4.34±4.41 % and -3.74±4.03 %, respectively. Relatively higher deviations of -12.73±6.23 % and 11.84±9.56 % were reported for the CO estimates.

VIII. DISCUSSION

In the present study, we implemented and assessed a novel method for predicting cardiac output and central systolic blood pressure based on noninvasive measurements of peripheral (brachial) pressure and pulse wave velocity. The method is based on the adjustment of a generic 1-D arterial model using the noninvasive recordings of the peripheral cuff-based systolic and diastolic blood pressures and carotid-to-femoral pulse wave velocity, which are easily obtained in a clinical setting. The one-dimensional model of the arterial tree, which has been thoroughly validated in vivo [22], [24], provides realistic flow and pressure waveforms. An optimization process was developed in order to fuse the computational model with the measurement data. We adjusted arterial model parameters such that model predictions fit the noninvasive recordings and thus, hopefully, render the generic model closer to a patient-specific model. This study demonstrated that creating a version of the generalized CV model closer to each patient's standards can potentially enhance the performance of the CO and cSBP prediction.

This article has been accepted for publication in a future issue of this journal, but has not been fully edited. Content may change prior to final publication. Citation information: DOI 10.1109/JBHI.2019.2956604, IEEE Journal of Biomedical and Health Informatics

Patient-specific models of the human vasculature are confronted with significant challenges that pertain to the unique characteristics of each individual. Geometry, in particular, cannot be completely defined for each arterial segment throughout the vasculature. In this study, the geometry of an individual was approximated by using data from a previously published study [34]. These data allowed for an estimation of the aortic size without the need for additional complicated or costly measurements. As anticipated, the aortic size approximation slightly deviated from the actual aortic dimension. However, having at our disposal the aortic diameter values (directly measured from echocardiography), we observed that the approximated diameter of the ascending aorta did not differ significantly from the true measured values (the difference was equal to 0.25±0.44 cm).

Peripheral noninvasive measurements proved to be adequate to adjust the arterial tree model and were demonstrated to be informative to predict aortic hemodynamics. CO and cSBP estimates were found to be in good agreement with the reference methods. Fig. 10 shows an aortic pressure waveform as resulted from the 1-D model. The model-derived aortic pressure wave bears all the characteristic details and shape of a physiological pressure signal. This observation further strengthens the physiological relevance of our results. To our knowledge, this novel work constitutes the first method that makes use of only three easily obtained inputs (e.g., noninvasive brSBP and brDBP, and PWV) to successfully adjust a 1-D generic arterial tree model and accurately predict hemodynamics at the aortic root (e.g., CO, cSBP). The fusion of clinically relevant noninvasive data with theory-based modeling avoids simplified assumptions that have been proposed by previous studies [18], [50]. Additionally, it should be noted that the clinical application of the proposed framework is highly facilitated by the fact that PWV can be routinely measured in clinical practice and has been identified as an independent predictor of cardiovascular disease [51]–[53], especially when it can be translated in conjunction with pressure measurements.

We performed an identifiability analysis as proposed by Brun *et al.* in order to identify the most sensitive parameters that drive the variability in the model output (i.e., brSBP, brDBP, and cf-PWV). This analysis can be very informative to guide the strategy for inverse problem-solving. The sensitivity matrix demonstrated that Q_{max} was the most sensitive determinant of the model output, which may be explained from the fact that aortic flow serves as the proximal boundary condition. Total peripheral resistance, T_{period} and arterial compliance followed. The sensitivity to T_{period} was directly addressed by exploiting the HR information. The high sensitivities of compliance and resistance can most likely be attributed to our selection of the model outputs, namely brachial SBP and DBP, and thus PP and MAP. Arterial compliance is a major determinant of PP [54] and total peripheral resistance dictates MAP. [55].

The mitigation of errors that are inevitably present in clinical measurements challenges the reliability of oscillometric devices. The majority of automatic cuff devices for measuring blood pressure are based on generalized models to estimate blood pressure from an oscillogram [56]. This can limit the accuracy of the device in a certain pressure range. A noteworthy approach has been proposed by Liu *et al.* [57]. They used a physiologic model in conjunction with model fitting [58]. The method has achieved to maintain blood pressure estimation accuracy whereas it was proven to be less sensitive to common physiologic deviations in the oscillogram. Here, artificial errors in brSBP and cf-PWV measurements were manually introduced in a discrete way in order to study the effect of each error on the predictions. However, it should be emphasized that measurements errors in brSBP and cf-PWV may also happen concurrently and be highly interdependent.

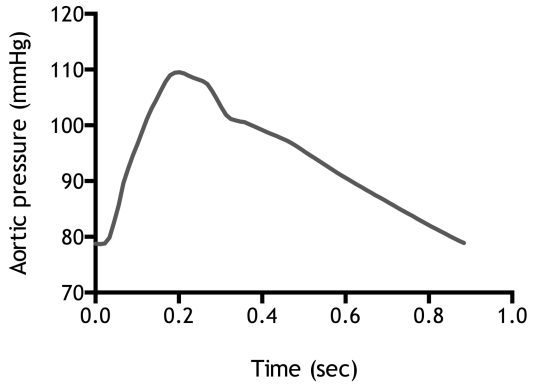

Fig. 10. Arbitrary aortic pressure waveform that was yielded from the 1-D arterial tree solver.

The sensitivity analysis in measurements' errors in brSBP and cf-PWV demonstrated evidence that the CO and cSBP predictions are expected to be more sensitive to errors in brSBP than to errors in cf-PWV. The cSBP prediction seems to be determined mainly from the brSBP information, while brSBP is rather sensitive to the resistance (sensitivity matrix, Fig. 2) that dictates the mean blood pressure. The strong sensitivity of cSBP estimation to brSBP errors is to be expected, since the input brSBP and the estimated cSBP are strongly related to mean blood pressure, which is practically the same in both central and peripheral arterial sites.

cf-PWV, on the other hand, is related to arterial compliance, which is a weaker determinant of stroke volume and cardiac output, compared to arterial resistance and by extension to mean pressure, as also described in earlier work by Stergiopulos *et al.* [59]. In our analysis, this is clearly demonstrated in the scaled sensitivity matrix (Fig. 2); the sensitivity between cf-PWV and Q_{max}, and thus CO, is approximately 2.5 times smaller (equal to 0.42) compared to the sensitivity between brSBP and Q_{max} (equal to 1.00).

In order to evaluate the method's predictions, data from Mobil-O-Graph device were used. However, SphygmoCor data were also available and, therefore, we additionally compared our method's estimates using the data from the SphygmoCor device. Overall, a better performance was observed when pressure data from Mobil-O-Graph were used. It is possible that the discrepancies in CO and cSBP estimations between the two office devices may be attributed to differences between the two measurement techniques. First, differences exist in the technique of signal acquisition as well as the arterial site of recording; Mobil-O-Graph uses oscillometry at the brachial artery level and SphygmoCor uses applanation tonometry at the radial or carotid artery. Furthermore, differences exist in the computational method of central blood pressure derivation; Mobil-O-Graph applies the ArcSolver as previously described whereas SphygmoCor applies generalized transfer function [18]. SphygmoCor applies generalized transfer function while

Mobil-O-Graph the ArcSolver, previously described in [60] and [61] . The central aortic pressure derived from Mobil-O-Graph is simultaneously recorded with the brachial pressure. In contrast, SphygmoCor uses a generalized transfer function to transform the radial pressure wave into aortic pressure wave [50]. Since brachial pressure is the one that drives the optimization process, Mobil-O-Graph's simultaneous brachial and central pressures acquisition may potentially lead to a more accurate aortic-to-peripheral PP amplification and thus more accurate prediction. Additionally, SphygmoCor's generalized transfer function is likely to deviate from our partially individualized method at a greater extent than Mobil-O-Graph's "per patient" scheme. Finally, differences in measurement accuracy between the two apparatuses may be also due to different calibration methods [62].

Part of the state of the art has focused on the improvement of the already available generalized TFs. Swamy *et al.* have presented a work on an adaptive GT using information on the wave propagation delay time between aortic and peripheral pressure waves [63]. However, this information was obtained using prior knowledge of the aortic flow. Some of the previous authors have proposed an improved adaptive GT using arterial wave transmission and reflection coefficient information [64]. Their results have showed significant accuracy improvement in cSBP estimations (RMSE equal to 3.43 mmHg), especially in patients with low PP amplification.

Hahn *et al.* have introduced a novel approach on the central aortic pressure wave from measured peripheral pressure wave by employing an individualized transmission line (TL) model [65]. The method was evaluated on swine data and achieved a high correlation of 0.92 between predicted aortic SBP and the reference aortic SBP. Nevertheless, the use of a TL model may be regarded as a simplification due to the actual curvature of the arterial line and the multiple reflection sites that may not be accurately described by a lumped terminal impedance. Moreover, the methods presented above employ a single pressure waveform and thus, the individualization is considered to be more simplified compared to a technique that fuses multiple noninvasive measurements.

Approaches comparable to ours have been developed to address the challenges of patient-specific hemodynamic monitoring. Tosello *et al.* [66] have proposed a new technique for determining central blood pressure using a multiscale mathematical model which is adjusted based on age, height, weight, brachial pressure, left-ventricular end-systolic and end-diastolic volumes and aortic pulse wave velocity. The estimation derived from their method presented low performance (significant overestimation of 7.8 mmHg for cSBP prediction) when compared against data from the SphygmoCor device. In their work, a large number of input variables are needed, including also central qualities (e.g., end-systolic and end-diastolic volumes). Here, however, cSBP can be predicted with a higher accuracy and by using fewer input parameters for the partial individualization of the model. Therefore, this simplifies the measurement process and potentially decreases the total cost of monitoring. Recently, Guala *et al.* published a validation of the same multiscale model using invasive catheter data [67]. Their model provided an underestimation of both central systolic and diastolic pressure values; the difference between the invasive aortic pressure and the model-derived estimates was 4.30±16.70 mmHg for central systolic pressure and 3.80±10.40 mmHg for central diastolic pressure. Validation using invasive data should be conducted for our proposed methodology, so as to be able to perform a fair comparison between the performance of the two models.

Additionally, important cardiovascular risk predictors have recently been estimated from the fusion of multiple noninvasive measurements (i.e., pulse pressure waveforms at the arm and the ankle) [68]. The method provides predictions of central SBP and pulse pressure (PP), PP amplification, and pulse transit time. RMSE for cSBP was reported to be rather low (1.99 mmHg). An advantage of the technique is that it also yields the entire central pressure waveform. Nevertheless, the use of a lumped-parameter model to describe the arterial tree may not be sufficient for considering the intermediate reflections between the central and the distal arterial site. Hence, this may be considered as a simplification when compared to a complete model of the systemic circulation.

A particularly interesting study was performed by Swamy *et al.* [69]. They estimated CO using peripheral pressure waves from multiple arterial sites, is of particular interest. In the proposed methodology, the aortic pressure wave is computed by applying a multichannel blind system identification algorithm [70]. The concept is based on the assumption that an arterial path between two arterial sites can be described by a transfer function of a finite impulse response (FIR) filter. The filter parameters were defined through a deconvolution algorithm. Subsequently, CO was estimated via fitting a Windkessel model to the computed aortic pressure wave. The lumped parameters of the Windkessel model (compliance and resistance) were calculated by extracting the time constant from the aortic pressure wave. Although this method illustrated an effective way of identifying CO (with a normalized RMSE of 12.9 %), it constitutes a relatively simplified approach which is based on a mathematical transfer function with less physiological information on the patient-based cardiovascular system in comparison to a complete model of systemic circulation.

Fazeli and Hahn have also proposed an improved Windkessel approach for individualized CO and total peripheral resistance (TPR) estimation [71]. Their approach is based on "tuning" a WK model using measurements of systolic, diastolic, and mean arterial blood pressure. The method outperformed the standard Windkessel method (prediction improved by 16.00 %) providing also an optimal patient- and time-specific time constant that is needed to estimate CO and TPR. A limitation of the study pertains to the simple linear model that was used to associate pressure and arterial compliance. This may be far from the actual highly nonlinear relationship between the two [72] and may affect the validity of the method when applied on a wider range of pulse pressure values.

A. *Limitations*

A number of limitations need to be considered. The gold standard technique for central aortic pressure is an invasive, catheter-based measurement. In this study, evaluation was conducted using central aortic pressure waves obtained from the Mobil-O-Graph device. Although the Mobil-O-Graph has been successfully validated in the past [44], significant errors may be present in the Mobil-O-graph estimations. Therefore, the validation presented here is only of relative and limited

value. It cannot be used to demonstrate any potential advantage in comparison to the existing generalized mathematical models. Similarly, the reference method used for aortic flow was transcutaneous echocardiography, which can only allow us to conclude that the prediction of this method is a fair estimate of the true value. Future studies using gold standard invasive measurement techniques are required for full validation of the proposed method. From an ethical perspective, it was not possible to perform invasive measurements in the context of a validation study.

Another limitation lies in the small sample size of older subjects who exhibit high PWV values. Also, the subject cohort is quite uniform in terms of PP (e.g., standard deviation of PP equal to 4 mmHg). This does not allow us to assess how well the method adapts to large variations in PP. To further enhance the robustness of the proposed method, validation on a larger population (including a larger number of patients older than 50 years and a wider range of PP levels) should be performed.

Furthermore, the integration of previously published data in the adjustment of arterial diameter leads to an "average" version of the 1-D cardiovascular model in terms of geometric configuration. Even if we tune the model with the patient-specific measurements that we have at our disposal, the patient-specific character of the method cannot be entirely justified. However, a fully personalized model would not be possible, since this would require us to obtain numerous noninvasive and invasive measurements for every individual. Since CO is known to be particularly dependent on arterial geometry measurements [73], individualized CO prediction still remains a challenge.

In addition, the use of previously published data on HR-related systolic duration leads to an approximation of the aortic flow wave. However, the difference between the approximated $T_{systole}$ and the actual $T_{systole}$ (derived from the reference ultrasound aortic flows) was found to be -10.05±6.72 ms and thus not very considerable. Furthermore, the sensitivity analysis demonstrated that the model outputs were less sensitive to changes in $T_{systole}$ (Fig. 2). When the actual systolic duration was used as an input to the model, the CO and cSBP predictions were improved by 0.84 % and 0.63 %, respectively. As anticipated, the more information is embedded into the system, the more accurate our predictions become. However, our assumptions do not seem to significantly underestimate the prediction capacity of our model in the study population.

Moreover, we should comment that the aortic flow wave that we imposed as a proximal boundary condition had a constant shape (only Q_{max}, T_{period}, and $T_{systole}$ were modified), while the systolic duration was defined as a relative approximation with respect to HR. These points also contribute to characterizing the model as partially patient-specific.

This study demonstrates the method's capacity to predict absolute CO for each subject. However, clinical research is particularly interested in monitoring CO changes within the same patient [74]; especially for patients in the intensive care unit [75]. Thus, another limitation pertains to the lack of available data to validate changes in the estimated CO within an individual. Our future work envisages the evaluation of our method on inter-patient changes in CO data.

Another potential limitation may be the inconvenience in acquiring cf-PWV. Cf-PWV measurement requires sequential recording of the carotid and femoral pressure pulse via applanation tonometry [76], [77]. The measurement process also takes some time to obtain the two signals sequentially, whereas it is intrusive in that it requires palpation of the femoral pressure pulse near the groin [78]. Alternatively, the volume-clamp technique [79] proposes the use of the finger pressure waveform for estimating cSBP and CO. Nevertheless, this technique excludes the arterial stiffness information embedded in cf-PWV which potentially enhances the physiological relevance of CO calculation.

Nobody can exclude that certain combinations of cardiac and arterial parameters may yield similar pressure and PWV values. We tested our method on a synthetic case of reduced contractility in the presence of increased total peripheral resistance and assessed its performance. Concretely, the cardiac contractility was reduced by decreasing the end-systolic elastance (Ees) by 20 % while total peripheral resistance was increased by 40 % in order to maintain pressure at normal levels. This yielded brachial SBP and DBP, and cf-PWV, which were isolated and used as input to the inverse method. After the optimization process, the estimated CO and cSBP for the case of reduced contractility were close to their real values (-0.21 % error in cSBP prediction and 3.30 % in CO prediction). Nevertheless, it is possible that there are extreme cases for which our algorithm may fall short in making an accurate prediction. Therefore, further investigation on the method's performance in such cases should be performed in order to evaluate the potential errors in a larger scale.

Finally, this method has been designed and applied on a healthy population. Hence, its applicability might be limited in the case of pathological conditions, such as aneurysm or aortic valve disease, where the relationship between input and output values is significantly modified and often poorly specified. Investigation of the method's performance on such populations could also be of particular interest.

IX. Conclusion

In conclusion, it was demonstrated that a generic 1-D model of the systemic circulation can be effectively adjusted to partially patient-specific standards using noninvasive measurements of peripheral cuff-based pressure and PWV. The in vivo evaluation suggests that this novel method predicts CO and cSBP with good accuracy and specificity. Further clinical validation against gold standards measurements remains to be performed in order to verify that the proposed technique may be employed for noninvasive CO and cSBP monitoring in the clinical setting.

References

[1] T. K. Waddell, A. M. Dart, T. L. Medley, J. D. Cameron, and B. A. Kingwell, "Carotid pressure is a better predictor of coronary artery disease severity than brachial pressure," *Hypertension*, vol. 38, no. 4, pp. 927–931, Oct. 2001.

[2] M. E. Safar *et al.*, "Central pulse pressure and mortality in end-stage renal disease," *Hypertension*, vol. 39, no. 3, pp. 735–738, Mar. 2002.

[3] H. Berkenstadt *et al.*, "Stroke Volume Variation as a Predictor of Fluid Responsiveness in Patients Undergoing Brain Surgery," *Anesthesia & Analgesia*, vol. 92, no. 4, pp. 984–989, Apr. 2001.

[4] M. McKendry, H. McGloin, D. Saberi, L. Caudwell, A. R. Brady, and M. Singer, "Randomised controlled trial assessing the impact of a nurse delivered, flow monitored protocol for optimisation of circulatory status after cardiac surgery," *BMJ*, vol. 329, no. 7460, p. 258, Jul. 2004.

[5] N. Lees, M. Hamilton, and A. Rhodes, "Clinical review: Goal-directed therapy in high risk surgical patients," *Crit Care*, vol. 13, no. 5, p. 231, 2009.

[6] A. Avolio, "Central aortic blood pressure and cardiovascular risk: a paradigm shift?," *Hypertension*, vol. 51, no. 6, pp. 1470–1471, Jun. 2008.

[7] L. Yang, B. Qin, X. Zhang, Y. Chen, and J. Hou, "Association of central blood pressure and cardiovascular diseases in diabetic patients with hypertension," *Medicine (Baltimore)*, vol. 96, no. 42, Oct. 2017.

[8] A. Song-Tao, Q. Yan-Yan, and W. Li-Xia, "The severity of coronary artery disease evaluated by central systolic pressure and fractional diastolic pressure," *N Am J Med Sci*, vol. 2, no. 5, pp. 218–220, May 2010.

[9] P. L. Marino, *The ICU book*, 2. ed. Baltimore: Lippincott Williams & Wilkins, 1998.

[10] X. Xiao, E. T. Ozawa, Y. Huang, and R. D. Kamm, "Model-Based Assessment of Cardiovascular Health from Noninvasive Measurements," *Annals of Biomedical Engineering*, vol. 30, no. 5, pp. 612–623, May 2002.

[11] S. Söderström, G. Nyberg, M. F. O'Rourke, J. Sellgren, and J. Pontén, "Can a clinically useful aortic pressure wave be derived from a radial pressure wave?," *British Journal of Anaesthesia*, vol. 88, no. 4, pp. 481–488, Apr. 2002.

[12] S. A. Hope, D. B. Tay, I. T. Meredith, and J. D. Cameron, "Use of arterial transfer functions for the derivation of aortic waveform characteristics," *J. Hypertens.*, vol. 21, no. 7, pp. 1299–1305, Jul. 2003.

[13] W. J. Stok, B. E. Westerhof, and J. M. Karemaker, "Changes in finger-aorta pressure transfer function during and after exercise," *Journal of Applied Physiology*, vol. 101, no. 4, pp. 1207–1214, Oct. 2006.

[14] B. Fetics, E. Nevo, C.-H. Chen, and D. M. Kass, "Parametric model derivation of transfer function for noninvasive estimation of aortic pressure by radial tonometry," *IEEE Transactions on Biomedical Engineering*, vol. 46, pp. 698–706, 1999.

[15] A. A. Udy, M. Altukroni, P. Jarett, J. A. Roberts, and J. Lipman, "A comparison of pulse contour wave analysis and ultrasonic cardiac output monitoring in the critically ill," *Anaesthesia and Intensive Care*, vol. 40, no. 4, pp. 631–637, Jul. 2012.

[16] J. R. C. Jansen, J. J. Schreuder, J. P. Mulier, N. T. Smith, J. J. Settels, and K. H. Wesseling, "A comparison of cardiac output derived from the arterial pressure wave against thermodilution in cardiac surgery patients," *British Journal of Anaesthesia*, vol. 87, no. 2, pp. 212–222, Aug. 2001.

[17] M. T. Ganter *et al.*, "Continuous cardiac output measurement by un-calibrated pulse wave analysis and pulmonary artery catheter in patients with septic shock," *J Clin Monit Comput*, vol. 30, no. 1, pp. 13–22, Feb. 2016.

[18] M. Karamanoglu, M. F. O'Rourke, A. P. Avolio, and R. P. Kelly, "An analysis of the relationship between central aortic and peripheral upper limb pressure waves in man," *Eur. Heart J.*, vol. 14, no. 2, pp. 160–167, Feb. 1993.

[19] M. Sugimachi, T. Shishido, K. Miyatake, and K. Sunagawa, "A new model-based method of reconstructing central aortic pressure from peripheral arterial pressure," *Jpn. J. Physiol.*, vol. 51, no. 2, pp. 217–222, Apr. 2001.

[20] A. C. Guyton and J. E. Hall, *Textbook of medical physiology*, 9th ed. Philadelphia: W.B. Saunders, 1996.

[21] P. Hallock and I. C. Benson, "STUDIES ON THE ELASTIC PROPERTIES OF HUMAN ISOLATED AORTA," *J Clin Invest*, vol. 16, no. 4, pp. 595–602, Jul. 1937.

[22] P. Reymond, Y. Bohraus, F. Perren, F. Lazeyras, and N. Stergiopulos, "Validation of a patient-specific one-dimensional model of the systemic arterial tree," *Am. J. Physiol. Heart Circ. Physiol.*, vol. 301, no. 3, pp. H1173-1182, Sep. 2011.

[23] J.-X. Wang, X. Hu, and S. C. Shadden, "Data-augmented modeling of intracranial pressure," *arXiv:1807.10345 [physics]*, Jul. 2018.

[24] S. Pagoulatou and N. Stergiopulos, "Evolution of aortic pressure during normal ageing: A model-based study," *PLOS ONE*, vol. 12, no. 7, p. e0182173, Jul. 2017.

[25] T. G. Papaioannou *et al.*, "First in vivo application and evaluation of a novel method for non-invasive estimation of cardiac output," *Med Eng Phys*, vol. 36, no. 10, pp. 1352–1357, Oct. 2014.

[26] P. Reymond, F. Merenda, F. Perren, D. Rüfenacht, and N. Stergiopulos, "Validation of a one-dimensional model of the systemic arterial tree," *Am. J. Physiol. Heart Circ. Physiol.*, vol. 297, no. 1, pp. H208-222, Jul. 2009.

[27] G. J. Langewouters, *Visco-elasticity of the Human Aorta in Vitro in Relation to Pressure and Age*. 1982.

[28] R. Holenstein, P. Niederer, and M. Anliker, "A viscoelastic model for use in predicting arterial pulse waves," *J Biomech Eng*, vol. 102, no. 4, pp. 318–325, Nov. 1980.

[29] K. Sagawa, H. Suga, A. A. Shoukas, and K. M. Bakalar, "End-systolic pressure/volume ratio: a new index of ventricular contractility," *Am. J. Cardiol.*, vol. 40, no. 5, pp. 748–753, Nov. 1977.

[30] Suga Hiroyuki and Sagawa Kiichi, "Instantaneous Pressure-Volume Relationships and Their Ratio in the Excised, Supported Canine Left Ventricle," *Circulation Research*, vol. 35, no. 1, pp. 117–126, Jul. 1974.

[31] Donald G. Watts and Douglas M. Bates, *Nonlinear Regression Analysis and Its Applications*. John Wiley & Sons, Inc, 1988.

[32] R. Brun, P. Reichert, and H. R. Künsch, "Practical identifiability analysis of large environmental simulation models," *Water Resources Research*, vol. 37, no. 4, pp. 1015–1030, 2001.

[33] T. Turányi, "Sensitivity analysis of complex kinetic systems. Tools and applications," *J Math Chem*, vol. 5, no. 3, pp. 203–248, Sep. 1990.

[34] A. Wolak *et al.*, "Aortic size assessment by noncontrast cardiac computed tomography: normal limits by age, gender, and body surface area," *JACC Cardiovasc Imaging*, vol. 1, no. 2, pp. 200–209, Mar. 2008.

[35] H. M. Mertens, H. Mannebach, G. Trieb, and U. Gleichmann, "Influence of heart rate on systolic time intervals: Effects of atrial pacing versus dynamic exercise," *Clinical Cardiology*, vol. 4, no. 1, pp. 22–27, Jan. 1981.

[36] Belsley, "Conditioning Diagnostics: Collinearilty and Weak Data in Regression," no. John wiley, New York, 1991.

[37] B. M. Kaess *et al.*, "Aortic Stiffness, Blood Pressure Progression, and Incident Hypertension," *JAMA*, vol. 308, no. 9, pp. 875–881, Sep. 2012.

[38] P. Reymond, N. Westerhof, and N. Stergiopulos, "Systolic hypertension mechanisms: effect of global and local proximal aorta stiffening on pulse pressure," *Ann Biomed Eng*, vol. 40, no. 3, pp. 742–749, Mar. 2012.

[39] E. Kimoto *et al.*, "Preferential Stiffening of Central Over Peripheral Arteries in Type 2 Diabetes," *Diabetes*, vol. 52, no. 2, pp. 448–452, Feb. 2003.

[40] P. Segers et al., "Three- and four-element Windkessel models: assessment of their fitting performance in a large cohort of healthy middle-aged individuals.," *Proceedings of the Institution of Mechanical Engineers, Part H: Journal of Engineering in Medicine*.

[41] Z. Lu and R. Mukkamala, "Continuous cardiac output monitoring in humans by invasive and noninvasive peripheral blood pressure waveform analysis," *Journal of Applied Physiology*, vol. 101, no. 2, pp. 598–608, Aug. 2006.

[42] R. B. P. de Wilde, J. J. Schreuder, P. C. M. van den Berg, and J. R. C. Jansen, "An evaluation of cardiac output by five arterial pulse contour techniques during cardiac surgery," *Anaesthesia*, vol. 62, no. 8, pp. 760–768, Aug. 2007.

[43] O. Vardoulis, T. G. Papaioannou, and N. Stergiopulos, "Validation of a novel and existing algorithms for the estimation of pulse transit time: advancing the accuracy in pulse wave velocity measurement," *American Journal of Physiology-Heart and Circulatory Physiology*, vol. 304, no. 11, pp. H1558–H1567, Jun. 2013.

[44] P. M. L. Franssen and B. P. M. Imholz, "Evaluation of the Mobil-O-Graph new generation ABPM device using the ESH criteria," *Blood Press Monit*, vol. 15, no. 4, pp. 229–231, Aug. 2010.

[45] W. Wei, M. Tölle, W. Zidek, and M. van der Giet, "Validation of the mobil-O-Graph: 24 h-blood pressure measurement device," *Blood Press Monit*, vol. 15, no. 4, pp. 225–228, Aug. 2010.

[46] S. Wassertheurer, C. Mayer, and F. Breitenecker, "Modeling arterial and left ventricular coupling for non-invasive measurements," *Simulation Modelling Practice and Theory*, vol. 16, no. 8, pp. 988–997, Sep. 2008.

[47] T. G. Papaioannou, A. D. Protogerou, K. S. Stamatelopoulos, M. Vavuranakis, and C. Stefanadis, "Non-invasive methods and techniques for central blood pressure estimation: procedures, validation, reproducibility and limitations," *Curr. Pharm. Des.*, vol. 15, no. 3, pp. 245–253, 2009.

[48] M. Karamanoglu, M. F. O'Rourke, A. P. Avolio, and R. P. Kelly, "An analysis of the relationship between central aortic and peripheral upper

limb pressure waves in man," *Eur. Heart J.*, vol. 14, no. 2, pp. 160–167, Feb. 1993.

[49] J. R. Womersley, *An elastic tube theory of pulse transmission and oscillatory flow in mammalian arteries*. Wright-Patterson Air Force Base, Ohio: Wright Air Development Center, Air Research and Development Command, 1957.

[50] C. H. Chen *et al.*, "Estimation of central aortic pressure waveform by mathematical transformation of radial tonometry pressure. Validation of generalized transfer function," *Circulation*, vol. 95, no. 7, pp. 1827–1836, Apr. 1997.

[51] H. J. Joo *et al.*, "The Relationship between Pulse Wave Velocity and Coronary Artery Stenosis and Percutaneous Coronary Intervention: a retrospective observational study," *BMC Cardiovascular Disorders*, vol. 17, no. 1, Dec. 2017.

[52] M. L. Muiesan *et al.*, "Pulse wave velocity and cardiovascular risk stratification in a general population: the Vobarno study," *J. Hypertens.*, vol. 28, no. 9, pp. 1935–1943, Sep. 2010.

[53] A. R. Khoshdel, S. L. Carney, B. R. Nair, and A. Gillies, "Better Management of Cardiovascular Diseases by Pulse Wave Velocity: Combining Clinical Practice with Clinical Research using Evidence-Based Medicine," *Clin Med Res*, vol. 5, no. 1, pp. 45–52, Mar. 2007.

[54] N. Stergiopulos and N. Westerhof, "Determinants of pulse pressure," *Hypertension*, vol. 32, no. 3, pp. 556–559, Sep. 1998.

[55] B. A. Greene, "CARDIAC OUTPUT AND TOTAL PERIPHERAL RESISTANCE IN ANESTHESIOLOGY: CLINICAL APPLICATIONS," *JAMA*, vol. 166, no. 9, pp. 1003–1010, Mar. 1958.

[56] C. R. Jones, K. Taylor, P. Chowienczyk, L. Poston, and A. H. Shennan, "A validation of the Mobil O Graph (version 12) ambulatory blood pressure monitor," *Blood Press Monit*, vol. 5, no. 4, pp. 233–238, Aug. 2000.

[57] J. Liu, H.-M. Cheng, C.-H. Chen, S.-H. Sung, J.-O. Hahn, and R. Mukkamala, "Patient-Specific Oscillometric Blood Pressure Measurement: Validation for Accuracy and Repeatability," *IEEE J Transl Eng Health Med*, vol. 5, p. 1900110, 2017.

[58] J. Liu *et al.*, "Patient-Specific Oscillometric Blood Pressure Measurement," *IEEE Trans Biomed Eng*, vol. 63, no. 6, pp. 1220–1228, 2016.

[59] N. Stergiopulos, J. J. Meister, and N. Westerhof, "Determinants of stroke volume and systolic and diastolic aortic pressure," *American Journal of Physiology-Heart and Circulatory Physiology*, vol. 270, no. 6, pp. H2050–H2059, Jun. 1996.

[60] W. Weiss, C. Gohlisch, C. Harsch-Gladisch, M. Tölle, W. Zidek, and M. van der Giet, "Oscillometric estimation of central blood pressure: validation of the Mobil-O-Graph in comparison with the SphygmoCor device," *Blood Press Monit*, vol. 17, no. 3, pp. 128–131, Jun. 2012.

[61] T. Weber *et al.*, "Validation of a brachial cuff-based method for estimating central systolic blood pressure," *Hypertension*, vol. 58, no. 5, pp. 825–832, Nov. 2011.

[62] T. G. Papaioannou *et al.*, "Accuracy of commercial devices and methods for noninvasive estimation of aortic systolic blood pressure a systematic review and meta-analysis of invasive validation studies," *J. Hypertens.*, vol. 34, no. 7, pp. 1237–1248, 2016.

[63] G. Swamy, D. Xu, N. B. Olivier, and R. Mukkamala, "An adaptive transfer function for deriving the aortic pressure waveform from a peripheral artery pressure waveform," *American Journal of Physiology-Heart and Circulatory Physiology*, vol. 297, no. 5, pp. H1956–H1963, Nov. 2009.

[64] M. Gao, W. C. Rose, B. Fetics, D. A. Kass, C.-H. Chen, and R. Mukkamala, "A Simple Adaptive Transfer Function for Deriving the Central Blood Pressure Waveform from a Radial Blood Pressure Waveform," *Sci Rep*, vol. 6, Sep. 2016.

[65] J. Hahn, A. T. Reisner, F. A. Jaffer, and H. H. Asada, "Subject-Specific Estimation of Central Aortic Blood Pressure Using an Individualized Transfer Function: A Preliminary Feasibility Study," *IEEE Transactions on Information Technology in Biomedicine*, vol. 16, no. 2, pp. 212–220, Mar. 2012.

[66] F. Tosello *et al.*, "Central Pressure Appraisal: Clinical Validation of a Subject-Specific Mathematical Model," *PLOS ONE*, vol. 11, no. 3, p. e0151523, Mar. 2016.

[67] A. Guala *et al.*, "Multiscale mathematical modeling vs. the generalized transfer function approach for aortic pressure estimation: a comparison with invasive data," *Hypertens. Res.*, vol. 42, no. 5, pp. 690–698, May 2019.

[68] Z. Ghasemi *et al.*, "Estimation of Cardiovascular Risk Predictors from Non-Invasively Measured Diametric Pulse Volume Waveforms via Multiple Measurement Information Fusion," *Scientific Reports*, vol. 8, no. 1, Dec. 2018.

[69] G. Swamy and R. Mukkamala, "Estimation of the aortic pressure waveform and beat-to-beat relative cardiac output changes from multiple peripheral artery pressure waveforms," *IEEE Trans Biomed Eng*, vol. 55, no. 5, pp. 1521–1529, May 2008.

[70] D. B. McCombie, A. T. Reisner, and H. H. Asada, "Laguerre-model blind system identification: cardiovascular dynamics estimated from multiple peripheral circulatory signals," *IEEE Transactions on Biomedical Engineering*, vol. 52, no. 11, pp. 1889–1901, Nov. 2005.

[71] N. Fazeli and J.-O. Hahn, "Estimation of cardiac output and peripheral resistance using square-wave-approximated aortic flow signal," *Front Physiol*, vol. 3, Jul. 2012.

[72] S. J. Marchais, A. P. Guerin, B. Pannier, G. Delavaud, and G. M. London, "Arterial Compliance and Blood Pressure:," *Drugs*, vol. 46, no. Supplement 2, pp. 82–87, 1993.

[73] A. Sahlén *et al.*, "Impact of aortic root size on left ventricular afterload and stroke volume," *European Journal of Applied Physiology*, vol. 116, no. 7, pp. 1355–1365, Jul. 2016.

[74] Y. Mehta, "Newer methods of cardiac output monitoring," *WJC*, vol. 6, no. 9, p. 1022, 2014.

[75] J. Huygh, Y. Peeters, J. Bernards, and M. L. N. G. Malbrain, "Hemodynamic monitoring in the critically ill: an overview of current cardiac output monitoring methods," *F1000Res*, vol. 5, p. 2855, Dec. 2016.

[76] A. Adji, M. F. O'Rourke, and M. Namasivayam, "Arterial stiffness, its assessment, prognostic value, and implications for treatment," *Am. J. Hypertens.*, vol. 24, no. 1, pp. 5–17, Jan. 2011.

[77] C. M. McEniery *et al.*, "Normal vascular aging: differential effects on wave reflection and aortic pulse wave velocity: the Anglo-Cardiff Collaborative Trial (ACCT)," *J. Am. Coll. Cardiol.*, vol. 46, no. 9, pp. 1753–1760, Nov. 2005.

[78] M. R. Nelson, J. Stepanek, M. Cevette, M. Covalciuc, R. T. Hurst, and A. J. Tajik, "Noninvasive Measurement of Central Vascular Pressures With Arterial Tonometry: Clinical Revival of the Pulse Pressure Waveform," *Mayo Clin Proc*, vol. 85, no. 5, pp. 460–472, May 2010.

[79] J. Y. Wagner, J. Grond, J. Fortin, I. Negulescu, M. Schöfthaler, and B. Saugel, "Continuous noninvasive cardiac output determination using the CNAP system: evaluation of a cardiac output algorithm for the analysis of volume clamp method-derived pulse contour," *J Clin Monit Comput*, vol. 30, no. 4, pp. 487–493, Aug. 2016.